



A Robust Power Control of a DFIG used in Wind Turbine Conversion System

www.ericjournal.ait.ac.th

Abdellah Boulouch^{*1}, Tamou Nasser⁺, Ahmed Essadki^{*},
Ali Boukhriss^{*} and Abdellatif Frigui^{*}

Abstract – This paper presents a robust power control of a doubly fed induction generator (DFIG) used in Wind Energy Conversion Systems (WECS) based on the active disturbance rejection control (ADRC) connected to the grid power. In this article we present the performance and robustness of ADRC compared to other controllers regulators such as the polynomial controller RST applied to powers control for DFIG. The proposed control strategy employs ADRC based on Extended State Observer (ESO) scheme to directly calculate the required rotor control voltage in order to eliminate the instantaneous errors of active and reactive powers. Listed in this paper are the advantage, performance and robustness of the Active Disturbance Rejection Control. First, we present a model of wind turbine and DFIG machine, then a synthesis of the controllers and their application in the DFIG power control. Simulation results on a 1.5MW grid-connected DFIG system are provided by MATLAB/Simulink.

Keywords – ADRC, DFIG, extended state observer, robust power control, wind turbine.

1. INTRODUCTION

Many research teams are interested in the study of Renewable Energy Source (RES). The wind energy is one of the subjects of these technological researches. The use of wind energy is expanding day by day, so many wind farms are in service worldwide. Although this energy source is inexhaustible and environmental friendly its cost remains high as well as its sensibility to grid parameters and its efficiency is still low compared to conventional sources [1], [2].

Among the most used generators in high power wind production, we find the Doubly Fed Induction Generator (DFIG). The stator of DFIG is directly linked to the power grid, on the other side the rotor is connected to the grid through back-to-back power electronic converter, the Figure 1 shows a wind energy conversion system based on DFIG connected to the grid [1], [2].

The advantage of this type of machine is the ability to operate over a large range of wind speed and reduces the size and cost of power converters [3], in fact the power transiting through the back to back converter is about 30%~40% of its rated power.

These last years, several researches are about the advanced and robust controllers such as RST, Sliding Mode Controller, Backstepping and Active disturbance Rejection Control ADRC to improve the DFIG's control and get the best reliable and stable power out of it.

However this type of controllers presents some limitations in case of grid defaults.

In this study, the control of rotor side converter RSC is based on ADRC controller which had enjoyed great success for its simple implementation and immunity against disturbances that may affect process [7]-[16].

In this article and after modelling the wind turbine and DFIG, we have established a vector control to control the active and reactive power using an ADRC controller. The aim of this work is to present this controller compared to other controllers such as RST polynomial controller, in order to evaluate the robustness and performance of this new regulator, with DFIG parameter variation and the limitation in case of grid fault (voltage dips). The following figure shows the main scheme of a regular system lead by an ADRC and a RST. Where;

Y_{ref} = Reference

Y = Output

d = Disturbance

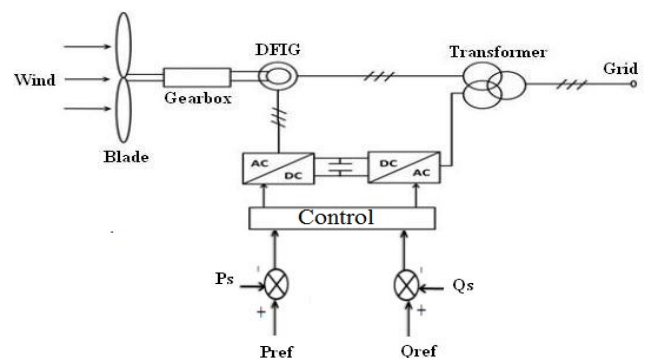


Fig. 1. Wind energy conversion system based on DFIG connected to the grid.

^{*}Electrical Engineering Laboratory, High school of education (ENSET), Mohammed V University, Medinat Al-irfane, Rabat, Morocco.

⁺Communication networks department of National High School for Computer Science and Systems (ENSIAS), Mohammed V University, Medinat Al-irfane, Rabat, Morocco.

¹Corresponding author:

Tel.: 00212662779347;

E-mail: abdellah.boulouch@um5s.net.ma.

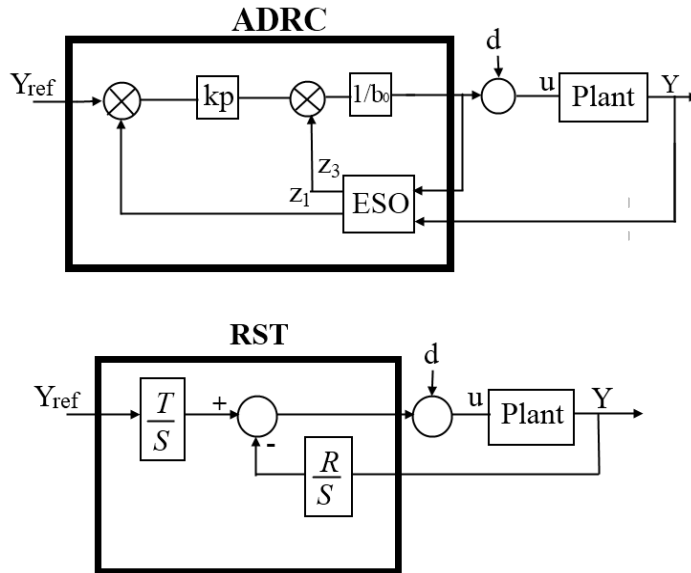


Fig. 2. Block diagram of the ADRC and RST controller.

2. TURBINE AND DFIG MODEL

The mechanical power transferred from the wind to the aerodynamic rotor is [8]:

$$P_{mt} = \frac{1}{2} \rho R^2 V^3 C_p(\lambda, \beta) \tag{1}$$

The input torque in the transmission mechanical system is:

$$T_t = \frac{\frac{1}{2} \rho R^2 V^3 C_p(\lambda, \beta)}{\Omega_t} \tag{2}$$

The power coefficient C_p of the wind turbine is given by the following formula [9]:

$$C_p(\lambda, \beta) = 0.51 \left(\frac{116}{\lambda i} - 0.4\beta - 5 \right) e^{\frac{-21}{\lambda}} + 0.0068\lambda \tag{3}$$

$$\frac{1}{\lambda_1} = \frac{1}{\lambda + 0.08\beta} - \frac{0.035}{\beta^3 + 1} \tag{4}$$

The mathematical model of the DFIG in the Park frame is written as follow [6]:

$$\begin{cases} V_{ds} = R_s I_{ds} + \frac{d\Phi_{ds}}{dt} - \omega_s \Phi_{qs} \\ V_{qs} = R_s I_{qs} + \frac{d\Phi_{qs}}{dt} + \omega_s \Phi_{ds} \\ V_{dr} = R_r I_{dr} + \frac{d\Phi_{dr}}{dt} - \omega_r \Phi_{qr} \\ V_{qr} = R_r I_{qr} + \frac{d\Phi_{qr}}{dt} + \omega_r \Phi_{dr} \end{cases} \tag{5}$$

$$\begin{cases} \Phi_{ds} = L_s I_{ds} + L_m I_{dr} \\ \Phi_{qs} = L_s I_{qs} + L_m I_{qr} \\ \Phi_{dr} = L_r I_{dr} + L_m I_{ds} \\ \Phi_{qr} = L_r I_{qr} + L_m I_{qs} \end{cases} \tag{6}$$

The electromagnetic torques is expressed as in [6]-[8]-[13]:

$$T_e = -\frac{3}{2} p \frac{L_m}{L_s} (\Phi_{ds} I_{dr} - \Phi_{qs} I_{ds}) \tag{7}$$

The active and reactive power is expressed as:

$$\begin{cases} P_s = V_{qs} I_{qs} + V_{ds} I_{ds} \\ Q_s = V_{qs} I_{ds} - V_{ds} I_{qs} \end{cases} \tag{8}$$

3. ACTIVE DISTURBANCE REJECTION CONTROL

The active disturbance rejection control (ADRC) was developed by Han [10]-[11]. It is designed to deal with systems having a large amount of uncertainty in both the internal dynamics and external disturbances [5]-[12].

The total disturbance of the proposed ADRC is particularly defined as an extended state of the system (DFIG in this case); and estimated using a state observer, known as the extended state observer (ESO) [5]-[14].

The ADRC is built from the transient profile; the total disturbance was estimated using an extended state observer and the feedback state error controller.

To illustrate the principle of the ADRC, we consider the case of a first order system.

$$\frac{dy(t)}{dt} = -\frac{1}{T} y(t) + bu(t) \tag{9}$$

Where:

b parameter to estimate.

u and y are input and output variables.

We consider :

$$\begin{cases} b = b_0 + \Delta b \\ b_0 = \frac{K}{T} \end{cases} \quad (10)$$

b_0 is known part of b ,

Δb is variation in system parameters,

K is the gain and T is a constant of the system.

When the external disturbances are added to the system, it becomes:

$$\begin{cases} \frac{dy(t)}{dt} = -\frac{1}{T}y(t) + \frac{1}{T}d(t) + \Delta bu(t) + b_0u(t) \\ \frac{dy(t)}{dt} = f(y, d, t) + b_0u(t) \end{cases} \quad (11)$$

Where:

$$f(y, d, t) = -\frac{1}{T}y(t) + \frac{1}{T}d(t) + \Delta bu(t) \quad (12)$$

$f(y, d, t)$ represents the internal and external disturbance .

The goal behind this synthesis is the estimation and compensation of f . In an augmented state form, the Equation (12) can be written as:

$$\begin{cases} \dot{x}_1 = x_2 + b_0u \\ \dot{x}_2 = h \\ y = x_1 \end{cases} \quad \text{Where } h = \dot{f} \quad (13)$$

In Matrix form

$$\begin{cases} \dot{x} = Ax + b_0Bu + Eh \\ y = Cx \end{cases} \quad (14)$$

Where:

$$A = \begin{pmatrix} 0 & 0 \\ 0 & 0 \end{pmatrix} \quad B = \begin{pmatrix} b_0 \\ 0 \end{pmatrix} \quad C = \begin{pmatrix} 1 & 0 \end{pmatrix} \quad \text{and} \quad E = \begin{pmatrix} 0 \\ 1 \end{pmatrix} \quad (15)$$

Being that the Equation (13) is now a state in the extended state model, the observer will be able to estimate the derivatives of y and f . This observer known as an Extended State Observer (ESO) is constructed as:

$$\begin{cases} \dot{\hat{x}} = Ax + b_0Bu + L(y - \hat{y}) \\ \hat{y} = Cx \end{cases} \quad (16)$$

Where $L = \begin{pmatrix} \beta_1 \\ \beta_2 \end{pmatrix}$ is the observer gain vector. To simplify the tuning process, the observer gains are parametrized as [5]:

$$L = \begin{pmatrix} 2w_0 \\ w_0^2 \end{pmatrix} \quad (17)$$

Where, w_0 is the bandwidth of the observer determined by the pole placement technique [11]. The estimate is

more precisely by increasing the bandwidth of the observer; however, a wide bandwidth increases the sensitivity to noise. In practice, a compromise is made between the speed at which the observer tracks the states and its sensitivity to sensor noise. With a properly designed ESO, z_1 and z_2 are tracking respectively y and f . The control law is given by:

$$u = \frac{u_0 - z_2}{b_0} \quad (18)$$

The original plant in Equation (11) is reduced to a unit gain integrator.

$$\frac{dy(t)}{dt} = (f - z_2) + u_0 \approx u_0 \quad (19)$$

This can be controlled by a simple proportional controller.

$$u_0 = K_p(r - z_1) \quad (20)$$

Where, r is the input signal reference to track.

The controller tuning is chosen as $k_p = w_c$, where w_c is the desired closed loop frequency [15]. The combination of linear ESO and the controller is the linear ADRC. In general, we choose $w_0 = 3 \sim 7w_c$, and consequently, w_c is the only tuning parameter. Figure 3 represents the implementation of the ADRC.

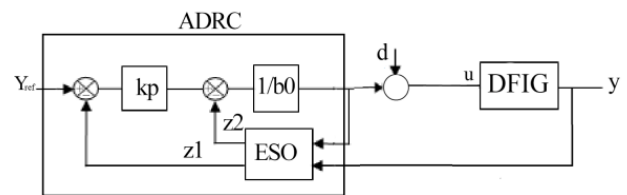


Fig. 3. Architecture of ADRC controller.

4. CONTROL STRATEGY

In this study we use a vector control of DFIG based on stator field oriented (SFO) to simplify the study of the power control strategy, by setting the stator field aligned with d-axis [6]-[16]. We have:

$$\Phi_{sq} = 0 \quad \text{and} \quad \Phi_{sd} = \Phi_s \quad (21)$$

In this case the torque becomes:

$$T_e = -\frac{3}{2}p \frac{L_m}{L_s} (\Phi_{ds} I_{dr}) \quad (22)$$

This electro-mechanic torque and the reactive power depend only on the q-axis rotor current; the machines used in wind conversion are usually high power so we can neglect the stator resistance R_s [16]. We can write:

$$\begin{cases} \Phi_{ds} = \Phi_s = L_s I_{ds} + L_m I_{dr} \\ \Phi_{qs} = 0 = L_s I_{qs} + L_m I_{qr} \end{cases} \quad (23)$$

and

$$\begin{cases} V_{ds} = 0 \\ V_{qs} = V_s = \omega_s \Phi_{ds} \end{cases} \quad (24)$$

The statoric power is controlled by the rotor voltages V_{rd} and V_{rq} . It is an independent control of active and reactive powers. In the d-q reference frame, the power can be written as:

$$\begin{cases} P_s = V_{qs} I_{qs} + V_{ds} I_{ds} = -V_s \frac{L_m}{L_s} I_{qr} \\ Q_s = V_{qs} I_{ds} - V_{ds} I_{qs} = V_s \left(\frac{\Phi_s}{L_s} \right) - V_s \left(\frac{L_m}{L_s} \right) I_{dr} \end{cases} \quad (25)$$

$$\begin{cases} V_{dr} = R_r I_{dr} + \sigma L_r \frac{dI_{dr}}{dt} - g \omega_s \sigma L_r I_{qr} \\ V_{qr} = R_r I_{qr} + \sigma L_r \frac{dI_{qr}}{dt} - g \omega_s \sigma L_r I_{dr} + g \left(\frac{L_m V_s}{L_s} \right) \end{cases} \quad (26)$$

V_{rd} and V_{rq} are the two-phase components of the rotor voltages to impose on the DFIG to obtain the desired rotor currents. A judicious choice of regulators in the control loop and an adequate synthesis of these parameters will compensate the terms $(L_r - \frac{L_m^2}{L_s})$ coupling

between the two axes d and q [4].

From Equations (13) and (26) the following expressing of rotor are deduced:

$$\begin{cases} \frac{dI_{dr}}{dt} = \frac{V_{dr}}{\sigma L_r} - \frac{R_r I_{dr}}{\sigma L_r} + g \omega_s I_{qr} \\ \frac{dI_{qr}}{dt} = \frac{V_{qr}}{\sigma L_r} - \frac{R_r I_{qr}}{\sigma L_r} + g \omega_s I_{dr} - g \left(\frac{L_m V_s}{\sigma L_r L_s} \right) \end{cases} \quad (27)$$

At this stage, we can write:

$$\begin{cases} \frac{dI_{dr}}{dt} = f_d(I_{dr}, d, t) + b_0 u_d(t) \\ \frac{dI_{qr}}{dt} = f_q(I_{qr}, d, t) + b_0 u_q(t) \end{cases} \quad (28)$$

With:

$$\begin{cases} f_d = f_d(I_{dr}, d, t) + b_0 u_d(t) \\ f_q = f_q(I_{qr}, d, t) + b_0 u_q(t) \end{cases} \quad (29)$$

and:

$$\begin{cases} u_d = V_{dr}, b_0 = \frac{1}{\sigma L_r} \\ u_q = V_{qr}, b_0 = \frac{1}{\sigma L_r} \end{cases} \quad (30)$$

f_d and f_q are the total disturbance respectively affecting the rotor currents I_{dr} and I_{qr} . u_d and u_q are respectively the control inputs of the currents loops I_{dr} and I_{qr} , b_0 is the known part of the system parameters.

By choosing a suitable response time, we can easily determine the parameters k_p , β_1 and β_2 of the

ADRC controllers, so that the rotor currents follow their reference I_{drref} and I_{qrref} respectively given by Equation 25.

5. RST CONTROLLER

In this article the objective of choosing this type of regulator to show the performance of the ADRC is dictated by the simplicity of the RST regulator, this polynomial regulator is based on the robust pole placement method allowing the adjustment of output parameters (T_c , T_f). Those parameters represent respectively the control horizon and the filtering horizon [6]-[16].

However the full study synthesis of this regulator is not treated in this article as we will concentrate on the ADRC.

We considered a linear system with a transfer function:

$$\frac{B}{A} = \frac{L_m V_s}{L_s R_r + p L_s (L_r - \frac{L_m^2}{L_s})} \quad (31)$$

Regarding this transfer function, the degree of the denominator A is superior to the degree of the polynomial B, we can conclude that the system is stable. Furthermore, the degree of A is one and as we are in a clean regulator case, the robust pole placement method allows us to conclude that:

$$\begin{cases} \deg(R) = 1 \\ \deg(S) = 2 \\ \deg(D) = 3 \end{cases} \quad (32)$$

In order to enhance the speed and the robustness of the system we choose the polynomials poles as shown:

$$\begin{cases} D = CF \\ D = (s + \frac{1}{T_c})(s + \frac{1}{T_f})^2 \\ D = (s - p_c)(s - p_f)^2 \\ D = (s - 5p_A)(s - 20p_A)^2 \\ D = (s - 5 \frac{L_s R_r}{L_s (L_r - \frac{L_m^2}{L_s})})(s - 20 \frac{L_s R_r}{L_s (L_r - \frac{L_m^2}{L_s})}) \end{cases} \quad (33)$$

Using the expression of the Bezout equation:

$$D = AS + BR = CF \quad (34)$$

We end up with a system of four equations and four unknowns where the coefficients of the polynomial D are linked with the parameters of the polynomials R and S using Sylvester matrix.

$$\begin{cases} d_3 = a_1 s_2 \\ d_2 = a_1 s_1 \\ d_1 = a_0 s_1 + b_0 r_1 \\ d_0 = b_0 r_0 \\ T = r_0 \end{cases} \implies \begin{cases} s_2 = \frac{d_3}{a_1} \\ s_1 = \frac{a_1}{s_1} \\ r_1 = \frac{d_1 - a_0 s_1}{b_0} \\ r_0 = \frac{d_0}{b_0} \end{cases} \quad (35)$$

The final setting of the parameters is made through simulation in Matlab/Simulation in order to answer the needed requirements.

6. SIMULATION RESULTS AND DISCUSSION

To improve the power control of a DFIG by the Active Disturbance Rejection Control (ADRC), the simulations

on a 1.5MW DFIG wind turbine have been carried out using Matlab/Simulink.

The DFIG parameters used in this simulation are listed in Table I.

6.1 Reference Tracking

The machine speed is attached to 1600 rpm in ideal conditions, the active power reference P_{ref} is 0.75MW and 1.5MW (supply of power to the grid). The reactive power reference Q_{ref} is -0.5MVAR (inductive mode), 0.25MVAR (capacitive mode) and 0MVAR ($\cos\phi=1$). The ADRC parameters are listed in Table II.

The Figures 4 and 6 show the response of active and reactive power for DFIG and the error between the power and its reference by the ADRC and RST controller, the Figures 5 and 7 show the rotoric and statoric currents.

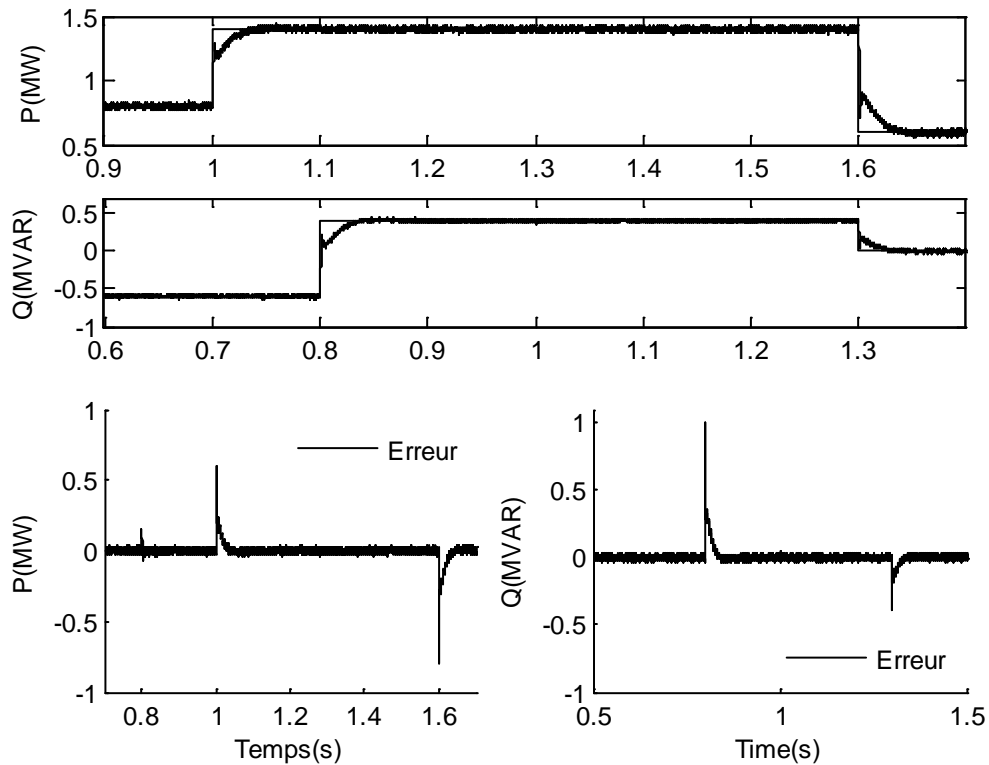


Fig. 4. Response of active and reactive power for DFIG by ADRC.

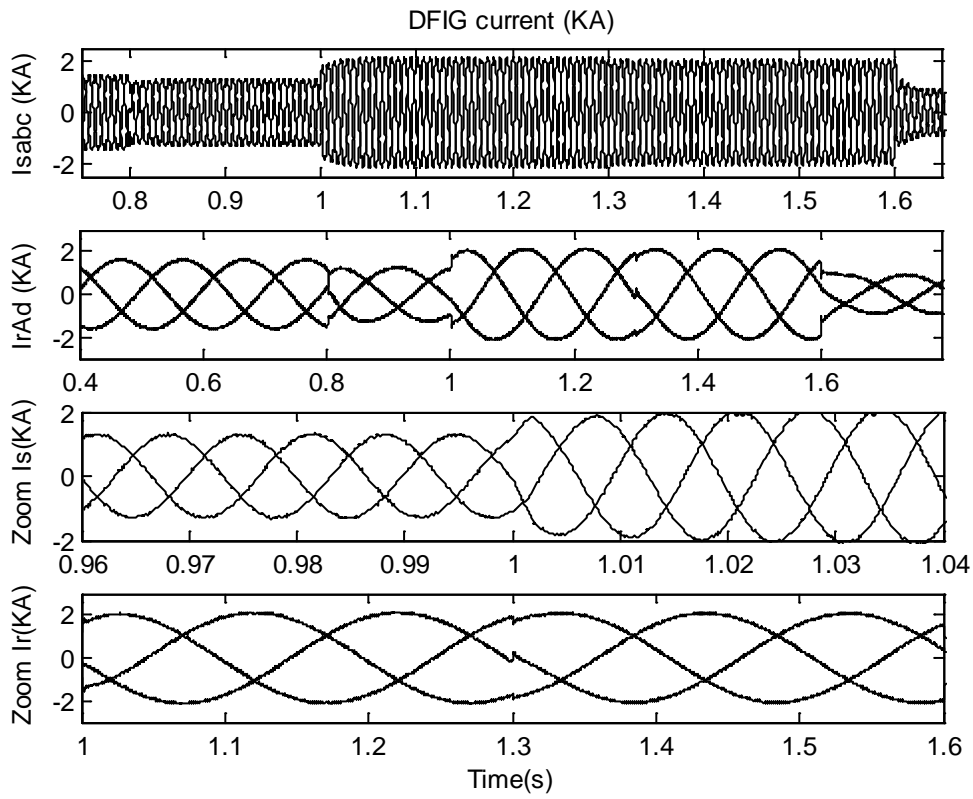


Fig. 5. DFIG current by ADRC

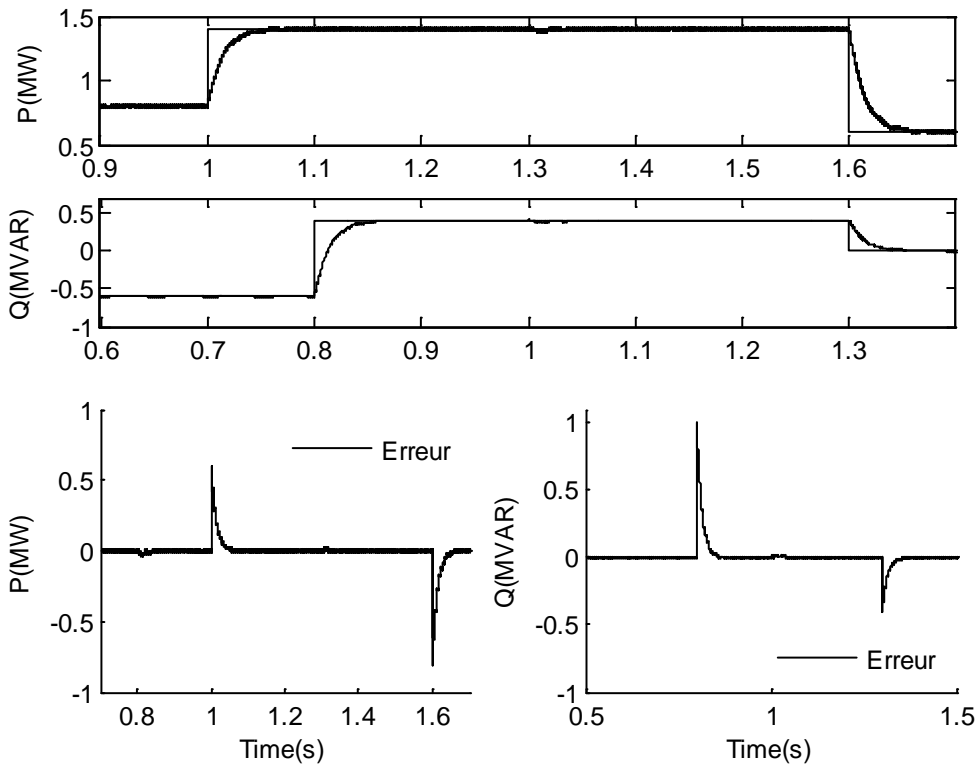


Fig. 6. Response of active and reactive power for DFIG by RST.

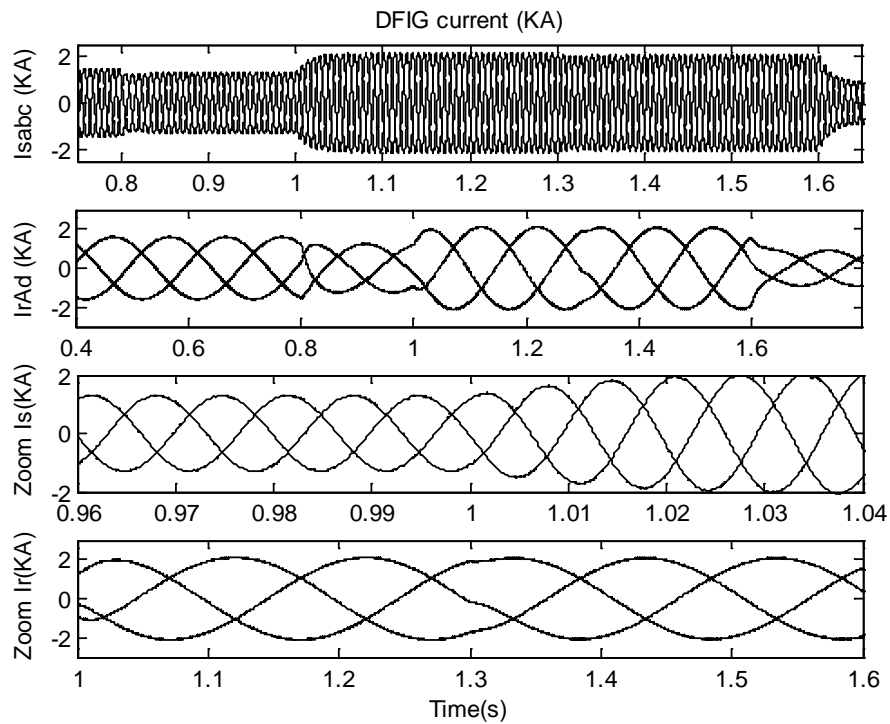


Fig. 7. DFIG current by RST.

6.2 Robustness Test

The characteristics of the electrical grid and the parameters of the DFIG are subject to changes driven by different physical phenomena, so our controller should provide good control whatever the variation of the generator parameters. In order to test the robustness of the controller we varied the rotor resistance R_r to $1.5R_r$, and the inductance value of the rotor and stator

decreased by 10% from its nominal value. Figures 8 and 9 show the effect of varying the parameters of the generator R_r , L_s , L_r and L_m on the response of the active and reactive power. Figure 10 shows the influence of a smaller grid voltage fault (15% and 65ms of dip voltage).

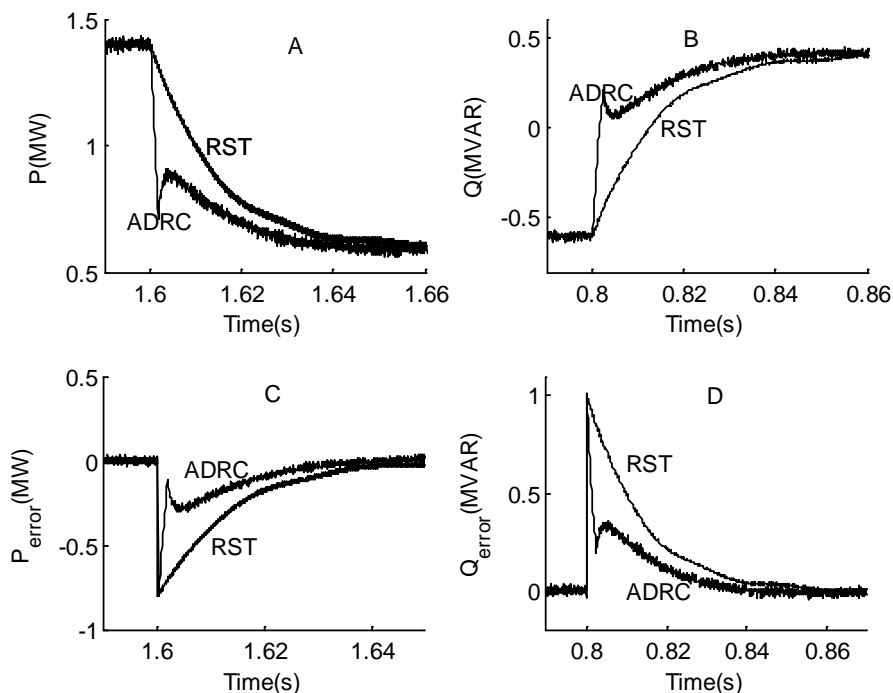


Fig. 8. Response of active and reactive power for DFIG with R_r variation by the ADRC and RST controller, A: active power, B: active reactive, C: active power error, D: active power error.

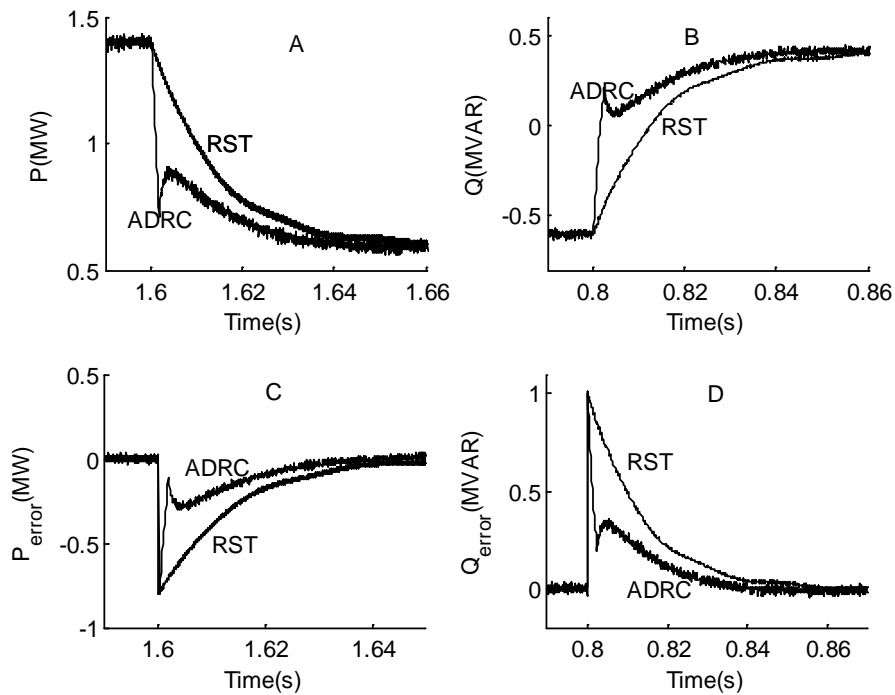


Fig. 9. Response of active and reactive power for DFIG with Inductance variation by the ADRC and RST controller, A: active power, B: active reactive, C: active power error, D: active power error.

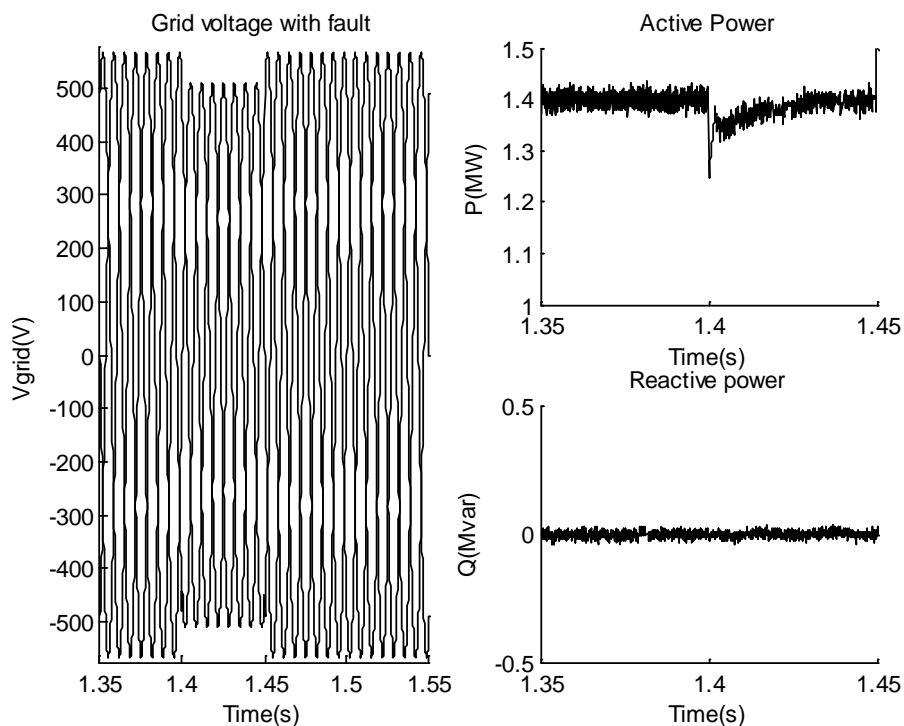


Fig. 10. Response of active and reactive power for DFIG during grid voltage fault (15% and 65ms of dip voltage).

7. RESULTS AND DISCUSSIONS

From the Figures 4, 5, 6 and 7 we can conclude a quicker response for ADRC, and the answers are without overshoots, no effect coupling between two axis compared to RST controller. The negative sign of the reactive power shows that the generator functions in

capacitive mode, for inductive mode the power becomes automatically positive. In the end, the decoupling between the two axes is perfectly respected.

For robustness test in Figure 8 and 9, we found that the ADRC is more robust, the response time is almost the same despite changes in the parameters of the DFIG.

Also from the simulation, due to increasing the resistance and inductance value we conclude that the ADRC loses its robustness in 1.78Rr of Rr variation and 17% of the inductances.

Although these values are far from reality, we can opt for a change in the machine or the rewinding.

On the other hand, the Figure 10 shows that the effectiveness of the control method proposed and the robustness of the ADRC is limited in the case of high variation of the stator voltage that follows major grid voltage disturbance with which the DFIG is directly connected through its stator circuit. In this study, the simulations results show also that the performances of the turbine are limited in the case of voltage dips with a high duration and large amplitude (Around 20%).

8. CONCLUSION

This paper has presented the improved power control of DFIG used in wind turbine by the active disturbance rejection control, after modeling the DFIG in the d and q axis, we have established a vector control of DFIG based on stator flux oriented, then the ADRC is synthesized and compared to a polynomial RST controller.

We have also presented the performance of the ADRC and RST and compared between them, the robustness of the controllers is evaluated and allows us to have a decoupling between active and reactive power thus independent control.

The simulation results show that the ADRC is much more efficient compared to RST, it also improves the performance of the power DFIG, and ensure some important strength despite the variation of the parameters of the DFIG.

The use of the ADRC has many advantages since it is based on the online rejection of the total uncertainties (compared to RST) and it doesn't require complete knowledge of the physical system.

We can conclude that the ADRC is an improved controller for DFIG power. This type of controller combines the effect of polynomial controller and the extended state observer which enhance its robustness.

We note that this control method based on the ADRC remains valid in certain conditions, other methods are used in the case of long duration and high amplitude voltage dips.

NOMENCLATURE

Cp	Power coefficient
ρ, β	Air density (1.225kg/m ³), pitch angle
v, λ	Wind speed (m/sec), tip speed ratio
G	Gain multiplier (1/35)
R	Rotor radius (35.25m)
Tem	Electromagnetic torque (Nm)
Vds, Vqs	Direct and quadratic stator voltages (V)
Vdr, Vqr	Direct and quadratic rotor voltages (V)

Ids, Iqs	Direct and quadratic stator currents (A)
Idr, Iqr	Direct and quadratic rotor currents (A)
Φ_{ds}, Φ_{qs}	Direct, quadratic stator flux (Wb)
Φ_{dr}, Φ_{qr}	Direct, quadratic rotor flux (Wb)
Ps, Qs	Active and reactive stator power
Pref, Qref	Reference active and reactive stator power
ω_s, ω_r	Synchronous and angular speed
g, p, θ_r	Slip, pole pair number, rotor position

REFERENCES

- [1] Sheikh M.R.I., Takahashi R. and Tamura J., 2011. Study on frequency fluctuations in power system with a large penetration of wind power generation. *International Energy Journal* 12(1): 77-86.
- [2] Chakrasali R.L., Nagaraja H.N., Sheelavant V.R., Murthy H.V. and Shalavadi B.S., 2012. Simulation and study of standalone hybrid grid (involving biogas, solar, wind and biodiesel –based generation). *International Energy Journal* 13(1): 45-52.
- [3] Abad G., Rodriguez M. and Poza J., 2007. Predictive direct power control of the doubly fed induction machine with reduced power ripple at low constant switching frequency. *IEEE International Symposium on Industrial Electronics, ISIE*, 1119-1124.
- [4] Boulahia A., Nabti K. and Benalla H., 2012. Direct power control for AC/DC/AC converters in doubly fed induction machine based wind turbine. *Journal of Theoretical and Applied Information Technology* (39).1.
- [5] Chakib R., Essadki A. and Echarkaoui M., 2014. Modeling and control of a wind system based on a DFIG by active disturbance rejection control. *International Review on Modelling and Simulations (IREMOS)*. 7(4): 626-637.
- [6] Belabbes A., Hamane B., Bouhamida M. and Draou A., 2012. Power control of a wind energy conversion system based on a doubly fed induction generator using RST and sliding mode controllers. *International Conference on Renewable Energies and Power Quality, Santiago de Compostela-Spain*.
- [7] Ardjoun S.A.E, Abid M., Alissaoui A. and Naceri A., 2011. A robust fuzzy sliding mode control applied to the double fed induction machine. *International Journal of Circuits, Systems and Signal Processing* (5) 4: 315-321.
- [8] Kerrouche K.D., Mezouar A., Boumediene L. and Belgacem K., Modeling and optimum power control based DFIG wind energy conversion system. 2014 *International Review of Electrical Engineering* 9 (1): 174-185.
- [9] Hilal M., Benchagra M., Errami Y., Maaroufi M. and Ouassaid M., 2011. Maximum power tracking of wind turbine based on doubly fed induction generator. *International Review on Modelling and Simulations* 4 (5): 2255-2263.

- [10] Han J., 2009. From PID to auto disturbances rejection control. *IEEE Transactions on Industrial Electronics*. (56) 3: 900-906.
- [11] Boukhriss A., Nasser T., Essadki A. and Boualouch A., 2014. Active disturbance rejection control for DFIG based wind farms under unbalanced grid voltage. *International Review on Modeling and Simulations* (7)1: 95-105.
- [12] Tian G. and A. Gao. 2007. Frequency response analysis of active disturbance rejection based control system. In *IEEE International Conference in Control Applications 2007*: 1595-1599.
- [13] Hu J. and Y. He. 2009. Modeling and enhanced control of DFIG under unbalanced grid voltage conditions. *Electric Power Systems Research* (79) 2: 273-281.
- [14] Zheng Q., 2009. On active disturbance rejection control: stability analysis and applications in disturbance decoupling control. *Ph.D. Dissertation*, Department of Electrical and Computer Engineering, Cleveland State University, Cleveland, USA.
- [15] Zheng Q., Chen Z. and Gao Z., 2009. A practical approach to disturbance decoupling control. *Control Engineering Practice* (17) 9: 1016-1025.
- [16] Boualouch A., Frigui A., Nasser T., Essadki A. and Boukhriss A., 2014. Control of a doubly-fed induction generator for wind energy conversion systems by RST controller. *International Journal of Emerging Technology and Advanced Engineering* (4) 8: 93-99.

APPENDIX

Table 1. DFIG Parameters.

Symbol	Quantity	Value
P	Rated power	1.5MW
Vs	Statoric voltage	690V – 50Hz
Vr	Rotoric voltage	389V-14Hz
Rs	Statoric resistance	0.012Ω
Rr	Rotoric resistance	0.021 Ω
Ls	Statoric inductance	0.0137 H
Lr	Rotoric inductance	0.0136H
Lm	mutual inductance	0.0135H
P	Pole pairs	2
F	The friction Coefficient	0.024N.m.s-1
J	The moment of inertia	1000 kg.m2

Table 2. ADRC and simulation parameters.

Symbol	Quantity	Value
kp	controller gain	130
b0	currents parameter	2530
wc	closed loop frequency	100
w0	Observer bandwidth	300
e	Fixed step size	10*1.65e ⁻⁵